J|A|C|S ARTICLES

Published on Web 09/20/2010

Oxygen Gas Sensing by Luminescence Quenching in Crystals of Cu(xantphos)(phen)$^+$ Complexes

Conor S. Smith,[†] Charles W. Branham,[‡] Brian J. Marquardt,[‡] and Kent R. Mann*,[†]

Department of Chemistry, University of Minnesota, Minneapolis, Minnesota 55455, and Applied Physics Laboratory, University of Washington, Seattle, Washington 98105

Received April 13, 2010; E-mail: krmann@umn.edu

Abstract: We have shown that crystals of the highly emissive copper(I) compounds [Cu(POP)(dmp)]tfpb, [Cu(xantphos)(dmp)]tfpb, [Cu(xantphos)(dipp)]tfpb, and [Cu(xantphos)(dipp)]pftpb, (where POP = bis[2-(diphenylphosphino)phenyl]ether; xantphos = 4,5-bis(diphenylphosphino)-9,9-dimethylxanthene; dmp = 2,9-dimethyl-1,10-phenanthroline; dipp = 2,9-diisopropyl-1,10-phenanthroline (dipp); tfpb$^-$ = tetrakis(bis-3,5-trifluoromethylphenylborate); and pftpb = tetrakis(pentfluorophenyl)borate) are oxygen gas sensors. The sensing ability correlates with the amount of void space calculated from the crystal structures. The compounds exhibit linear Stern−Volmer plots with reproducible K_{SV} constants from sample to sample; these results reinforce the observations that the sensing materials are crystalline and the sensing sites are homogeneous within the crystals. The long lifetime (~30 μs), high emission quantum yield (ϕ = 0.66), appreciable K_{SV} value (5.65), and very rapid response time (51 ms for the 95% return constant) for [Cu(xantphos)(dmp)]tfpb are significantly better than those for the [Cu(NN)$_2$]tfpb complexes studied previously and compare favorably with [Ru(4,7-Me2phen)$_3$](tfpb)$_2$, (K_{SV} = 4.76; 4,7-Me$_2$phen = 4,7-dimethyl-1,10-phenanthroline). The replacement of precious metals (like Ru or Pt) with copper may be technologically significant and the new compounds can be synthesized in one or two steps from commercially available starting materials. The strictly linear Stern−Volmer behavior observed for these systems and the absence of a polymer matrix that might cause variability in sensor to sensor sensitivity may allow a simple single-reference point calibration procedure, an important consideration for an inexpensive onetime limited use sensor that could be mass produced.

Introduction

Our group has been working with crystalline compounds[1−3] (such as [Ru(phen)$_3$]tfpb$_2$; phen = 1,10-phenanthroline; tfpb$^-$ = tetrakis(bis-3,5-trifluoromethylphenylborate)) that can sense oxygen gas by luminescence quenching. These compounds replace the typical polymer supports[4−8] with a crystal lattice that contains sufficient void space to allow diffusional oxygen quenching of a long-lived excited state. This type of crystalline material can mitigate technological problems such as the degradation of the polymer support matrix or luminophor[9] caused by the reactive oxygen species produced in the quenching events. These materials can also offer the possibility of reproducibility between sensors i.e. each sample of the pure solid will have the same sensing ability because of the crystallographic uniformity of the emission sites.

More recently we reported[10] the synthesis and study of new oxygen gas sensors that use a complex of Cu(I), an inexpensive, first row transition metal as the active sensing material to potentially decrease their price. We showed that crystalline [Cu(NN)$_2$]X (NN = 2,9 alkylsubstituted 1,10-phenanthroline, X$^-$ = BF_4^-, tfpb$^-$) complexes are photoluminescent oxygen sensors with high photochemical and thermal stability but they suffer from low emission quantum yields and relatively low sensitivity.[10] As a follow up of this work, our next goal was to design new Cu(I) compounds with improved quantum yields and lifetimes to aid detection and raise the K_{SV}'s (the Stern−Volmer quenching constant) for better oxygen sensing. The improved solution phase lifetimes reported for compounds in the [Cu(POP)(NN)]$^+$ family[11] (POP = bis[2-(diphenylphosphino)phenyl]ether; see Scheme 1) suggested that we should investigate these heteroleptic complexes as next generation candidates. The initially selected compound [Cu(POP)(dmp)]tfpb (**1**) (dmp = 2,9-dimethyl-1,10-phenanthroline), exhibits reasonable oxygen sensitivity but suffered from a relatively rapid photochemical degradation process. From this starting point we report the synthesis and study of a second series of new complexes of the form [Cu(xantphos)(NN)]X (xantphos = 4,5-

[†] University of Minnesota.
[‡] University of Washington.

(1) McGee, K. A.; Mann, K. R. *J. Am. Chem. Soc.* **2009**, *131*, 1896.
(2) McGee, K. A.; Marquardt, B. J.; Mann, K. R. *Inorg. Chem.* **2008**, *47*, 9143.
(3) McGee, K. A.; Veltkamp, D. J.; Marquardt, B. J.; Mann, K. R. *J. Am. Chem. Soc.* **2007**, *129*, 15092.
(4) Demas, J. N.; DeGraff, B. A.; Coleman, P. B. *Anal. Chem.* **1999**, *71*, 793A.
(5) Krenske, D.; Abdo, S.; Van Damme, H.; Cruz, M.; Fripiat, J. J. *J. Phys. Chem.* **1980**, *84*, 2447.
(6) Leventis, N.; Elder, I. A.; Rolison, D. R.; Anderson, M. L.; Merzbacher, C. I. *Chem. Mater.* **1999**, *11*, 2837.
(7) Lin, C.-T.; Sutin, N. *J. Phys. Chem.* **1976**, *80*, 97.
(8) Shi, L.; Li, B.; Yue, S.; Fan, D. *Sens. Actuators, B* **2009**, *B137*, 386.
(9) Carraway, E. R.; Demas, J. N.; DeGraff, B. A.; Bacon, J. R. *Anal. Chem.* **1991**, *63*, 337.
(10) Smith, C. S.; Mann, K. R. *Chem. Mater.* **2009**, *21*, 5042.
(11) Cuttell, D. G.; Kuang, S.-M.; Fanwick, P. E.; McMillin, D. R.; Walton, R. A. *J. Am. Chem. Soc.* **2002**, *124*, 6.

Scheme 1. Ligands Utilized in This Study

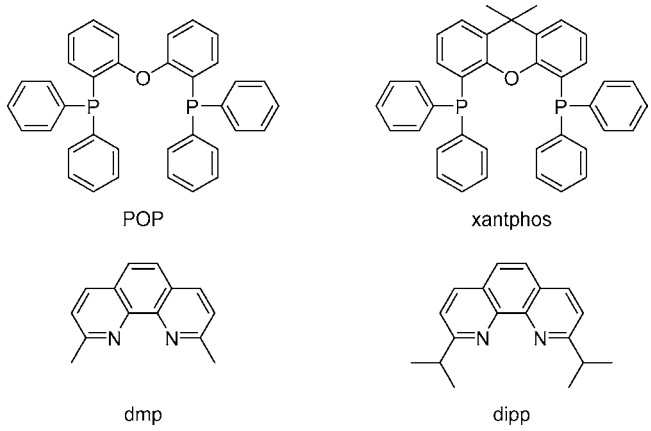

bis(diphenylphosphino)-9,9-dimethylxanthene) that exihibit higher photochemical stability, very high emission quantum yields and oxygen responsivity with rapid response times.

Experimental Section

General Considerations. $Cu(BF_4)_2 \cdot xH_2O$, bis[2-(diphenylphosphino)phenyl]ether (POP), and 4,5-bis(diphenylphosphino)-9,9-dimethylxanthene (xantphos) were purchased from Aldrich Chemical Co. and used as received. The solvents (dichloromethane, methanol, diethyl ether, acetonitrile, hexanes, and toluene) were obtained from commercial sources and either used without further purification or after drying with molecular sieves. The ligand 2,9-dimethyl-1,10-phenanthroline (dmp) was purchased from Aldrich, and potassium tetrakis(pentafluorophenyl) borate (Kpftpb) was purchased from Boulder Scientific Company. 2,9-diisopropyl-1,10-phenanthroline (dipp) was synthesized by a literature procedure.[12] Sodium(tetrakis(bis-3,5-trifluoromethyl(phenylborate))) (Natfpb) was available from a previous study.[13] $[Cu(CH_3CN)_4]BF_4$ was synthesized by a literature procedure.[14]

A 300 MHz Varian Unity NMR spectrometer was utilized to obtain the ^1H and ^{19}F NMR spectra. Chemical shifts are reported in units of ppm with an external reference to the residual proton resonance in deuterated dichloromethane or chloroform for ^1H NMR spectra and the internal $CFCl_3$ reference for the ^{19}F NMR. High-resolution mass spectrometry was carried out on a Bruker BioTOF II mass spectrometer.

Synthesis and Characterization. The $[Cu(POP)(dmp)]BF_4$ compound used in this study was synthesized as previously reported[11] by adding dmp to a solution of $[Cu(CH_3CN)_4]BF_4$ and POP in CH_2Cl_2 followed by precipitation of the salt with diethyl ether. The new BF_4^- salts containing the xantphos ligand were made by an analogous route. The metatheses to the $tfpb^-$ and $pftpb^-$ salts were carried out by adding a 1.2:1 ratio of Natfpb or Kpftpb to $[Cu(diphosphine)(phen\text{-}derivative)]BF_4$ in MeOH. Precipitation with water yielded pure compounds. The complete conversion by this metathesis route was confirmed by the presence of signals for $tfpb^-$ or $pftpb^-$ and the absence of signals for BF_4^- in the ^{19}F NMR of the products. The unexpected complexity of the ^1H NMR results obtained for the $[Cu(xantphos)(dipp)]X$ ($X = BF_4$, tfpb, and pftpb) compounds is discussed in the Supporting Information. The syntheses of $[Cu(POP)(dmp)]tfpb$ (**1**), $[Cu(xantphos)(dmp)]BF_4$ (**2a**), $[Cu(xantphos)(dmp)]tfpb$ (**2b**), $[Cu(xantphos)(dipp)]BF_4$ (**3a**), $[Cu(xantphos)(dipp)]tfpb$ (**3b**), and $[Cu(xantphos)(dipp)]pftpb$ (**3c**) are given below.

[Cu(POP)(dmp)]tfpb (1). Natfpb (0.0797 g, 0.09 mmol) was added to a methanol (30 mL) solution of $[Cu(POP)(dmp)]BF_4$ (0.070 g, 0.078 mmol). The yellow solid was precipitated by addition of water, filtered, and dried under vacuum yielding 0.083 g (64% yield). ^{1}NMR CD_2Cl_2 δ 8.28 (d, 2H $J = 8.4$), 7.804 (s, 2H), 7.717 (broad s, 8H), 7.553 (broad s, 4H), 7.518 (d, 2H $J = 8.4$), 7.343 (m, 2H), 7.242 (m, 10H), 6.996 (m, 16H), 2.437 (s, 6H) ^{19}F NMR (CD_2Cl_2) δ −63.521 (s, 24F) HRESIMS (M^+): calcd for $C_{50}H_{40}CuN_2OP_2$, 809.1906; found 809.1995.

[Cu(xantphos)(dmp)]BF_4 (2a). $[Cu(CH_3CN)_4]BF_4$ (0.054 g, 0.173 mmol) was added to a CH_2Cl_2 (20 mL) solution of xantphos (0.100 g, 0.173 mmol). Addition of dmp (0.036 g, 0.173 mmol) yielded a clear yellow solution. A bright yellow solid was precipitated upon addition of diethyl ether, filtered, and dried under vacuum yielding 0.1128 g (70% yield). ^{1}NMR CD_2Cl_2 δ 8.300 (d, 2H $J = 8.1$), 7.825 (s, 2H), 7.707 (dd, 2H $J = 7.8$,1.5), 7.515 (d, 2H $J = 8.4$), 7.253 (m, 6H), 7.055 (m, 16H), 6.938 (m, 4H), 2.291 (s, 6H), 1.775 (s, 6H) ^{19}F NMR (CD_2Cl_2) δ −154.125 (s, 4F).

[Cu(xantphos)(dmp)]tfpb (2b). Natfpb (0.0802 g, 0.09 mmol) was added to a methanol (20 mL) solution of [Cu(xantphos)(dmp)]BF_4 (0.0680 g, 0.073 mmol). The bright yellow solid was precipitated by addition of water, filtered, and dried under vacuum yielding 0.0746 g (59% yield). ^{1}NMR CD_2Cl_2 δ 8.288 (d, 2H, $J = 8.4$), 7.760 (s, 2H), 7.718 (bs, 8H), 7.669 (dd, 2H, $J = 7.8$, 1.5), 7.553 (bs, 4H), 7.458 (d, 2H, $J = 8.4$), 7.214 (m, 6H), 7.017 (m, 16H), 6.902 (m, 2H), 2.255 (s, 6H), 1.738 (s, 6H) ^{19}F NMR (CD_2Cl_2) δ −63.520 (s, 24 F) HRESIMS (M^+): calcd for $C_{53}H_{44}CuN_2OP_2$, 849.2219; found 849.2278.

[Cu(xantphos)(dipp)]BF_4 (3a). $[Cu(CH_3CN)_4]BF_4$ (0.054 g, 0.173 mmol) was added to a CH_2Cl_2 (20 mL) solution of xantphos (0.100 g, 0.173 mmol). Addition of dipp (0.046 g, 0.173 mmol) yielded a clear orange-yellow solution. A bright yellow solid was precipitated upon addition of diethyl ether, filtered, and dried under vacuum yielding 0.1380 g (80% yield). ^{1}NMR CD_2Cl_2 δ 8.388 (d, 1H $J = 8.7$), 8.243 (d, 1H $J = 8.1$), 7.796 (d, 2H $J = 8.4$), 7.700 (m, 4H), 7.581 (d, 1H $J = 8.4$), 7.519 (d, 1H $J = 8.7$), 7.437 (t, 2H $J = 7.2$), 7.250 (m, 12H), 7.046 (m, 4H), 6.793 (m, 4H), 6.708 (m, 4H), 3.697 (septet, 1H $J = 6.9$), 2.666 (septet, 1H $J = 7.2$), 2.005 (s, 3H), 1.470 (s, 3H), 1.071 (d, 6H $J = 6.9$), 0.1825 (d, 6H $J = 7.2$) ^{19}F NMR (CD_2Cl_2) δ −154.077 (s, 4F).

[Cu(xantphos)(dipp)]tfpb (3b). Natfpb (0.071 g, 0.08 mmol) was added to a methanol (20 mL) solution of [Cu(xantphos)-(dipp)]BF_4 (0.060 g, 0.060 mmol). The yellow solid was precipitated by addition of water, filtered, and dried under vacuum yielding 0.0457 g (46% yield). ^{1}NMR CD_2Cl_2 δ 8.345 (d, 1H $J = 8.7$), 8.210 (d, 1H $J = 8.1$), 7.715 (broad s, 8H), 7.701(m, 4H), 7.566 (d, 1H $J = 8.4$), 7.552 (broad s, 4H), 7.497 (d, 1H $J = 8.4$), 7.437 (t, 2H $J = 6.9$), 7.304 (m, 4H), 7.224 (m, 6H), 7.035 (m, 4H), 6.785 (t, 4H $J = 7.2$), 6.706 (m, 4H), 3.699 (septet, 1H $J = 6.6$), 2.670 (septet, 1H $J = 6.3$), 2.001 (s, 3H), 1.256 (s, 3H), 1.067 (d, 6H $J = 6.6$), 0.180 (d, 6H $J = 6.9$) ^{19}F NMR (CD_2Cl_2) δ −63.423 (s, 24F) HRESIMS (M^+): calcd for $C_{57}H_{52}CuN_2OP_2$, 905.2845; found 905.2842.

[Cu(xantphos)(dipp)]pftpb (3c). Kpftpb (0.0071 g, 0.01 mmol) was added to a methanol (5 mL) solution of **3a** (0.0070 g, 0.007 mmol). The light yellow solid was precipitated by addition of water, filtered, and dried under vacuum yielding 0.010 g (90% yield). ^{1}NMR CD_2Cl_2 δ 8.349 (d, 1H $J = 8.4$), 8.214 (d, 1H $J = 8.4$), 7.697 (m, 4H), 7.568 (d, 1H $J = 8.7$), 7.500 (d, 1H $J = 8.7$), 7.436 (m, 2H), 7.306 (m, 4H), 7.225 (m, 6H), 7.035 (m, 4H), 6.760 (m, 8H), 3.700 (septet, 1H $J = 6.3$), 2.670 (septet, 1H $J = 6.9$), 2.003 (s, 3H), 1.470 (s, 3H), 1.068 (d, 6H $J = 6.9$), −0.180 (d, 6H $J = 6.9$) ^{19}F NMR (CD_2Cl_2) δ −133.844 (s, 4F), −164.434 (t, 8F $J = 20.3$), −168.265 (t, 8F $J = 20.3$) HRESIMS (M^+): calcd for $C_{57}H_{52}CuN_2OP_2$, 905.2845; found 905.2837.

Single Crystal X-ray Crystallography. The crystal structures of compounds **1**, **2b**, **3b**, and **3c** were determined in this study. All

(12) Dietrich-Buchecker, C. O.; Marnot, P. A.; Sauvage, J. P. *Tetrahedron Lett.* **1982**, *23*, 5291.
(13) Exstrom, C. L.; Britton, D.; Mann, K. R.; Hill, M. G.; Miskowski, V. M.; Schaefer, W. P.; Gray, H. B.; Lamanna, W. M. *Inorg. Chem.* **1996**, *35*, 549.
(14) Dietrich-Buchecker, C.; Sauvage, J. P.; Kern, J. M. *J. Am. Chem. Soc.* **1989**, *111*, 7791.

Table 1. Crystallographic Data and Refinement Parameters

compound	**1**	**2b**	**3b**	**3c**
empirical formula	$C_{82}H_{52}BCuF_{24}N_2OP_2$	$C_{85}H_{56}BCuF_{24}N_2OP_2$	$C_{89}H_{64}BCuF_{24}N_2OP_2$	$C_{81}H_{52}BCuF_{20}N_2OP_2$
crystal color, morphology	yellow, block	yellow, plate	yellow, block	yellow, plate
crystal system	monoclinic	triclinic	triclinic	triclinic
space group	$P2_1$	$P\bar{1}$	$P\bar{1}$	$P\bar{1}$
a, Å	19.127(13)	15.289(2)	20.755(3)	11.0860(12)
b, Å	20.190(13)	16.539(2)	21.087(3)	17.2010(18)
c, Å	19.788(14)	17.019(2)	39.817(6)	19.803(2)
α, deg	90	102.685(2)	102.684(2)	76.694(2)
β, deg	93.402(23)	108.556(2)	90.297(3)	73.782(2)
γ, deg	90	97.253(2)	106.636(2)	88.210(2)
volume, Å^3	7628(7)	3889.9(9)	16246(4)	3526.4(6)
Z	4	2	8	2
formula weight, g mol^{-1}	1673.55	1713.61	1769.71	1585.54
density (calculated), g cm^{-3}	1.457	1.463	1.447	1.493
temperature, K	123(2)	123(2)	123(2)	173(2)
absorption coefficient, mm^{-1}	0.435	0.428	0.413	0.458
F(000)	3384	1736	7200	1608
θ range, deg	1.03−25.07	1.29−25.08	1.04−25.12	1.10−25.05
index ranges	$-22 \le h \le 22$	$-18 \le h \le 18$	$-24 \le k \le 24$	$-13 \le h \le 13$
	$-24 \le h \le 24$	$-19 \le k \le 19$	$-25 \le k \le 25$	$-20 \le l \le 20$
	$-23 \le l \le 23$	$-20 \le k \le 20$	$-47 \le l \le 47$	$-23 \le l \le 23$
reflections collected	56 974	38 903	160 490	34 822
independent reflections	26 506	13 776	57 495	12 443
weighting factors[a] *a*,*b*	0.0609	0.0461, 2.9848	0.1469, 32.590305	0.0531, 2.1772
max, min transmission	0.7452, 0.6435	0.94, 0.820337	0.7452, 0.6540	0.995, 0.872
data/restraints/parameters	26506/97/2113	13776/0/1089	57495/0/4395	12443/0/979
R_1, wR_2 [$I > 2\sigma(I)$]	0.0532, 0.1183	0.0380, 0.0920	0.0925, 0.2414	0.0455, 0.1051
R_1, wR_2 (all data)	0.0949, 0.1424	0.0578, 0.1052	0.1882, 0.3005	0.0903, 0.1279
GOF	1.006	1.015	1.057	1.063
largest diff. peak, hole, eÅ^{-3}	1.443, −0.479	0.426, −0.399	2.635, −0.789	0.722, −0.519

[a] $w = [\sigma^2(F_o^2) + (aP)^2 + (bP)]^{-1}$, where $P = (F_o^2 + 2F_c^2)/3$.

crystals were grown by slow evaporation of MeOH/H_2O solutions. Relevant crystallographic data are shown in Table 1, and details of the structure determinations are given in the Supporting Information. All of the data for these structure determinations were collected at the X-ray crystallographic laboratory (Department of Chemistry, University of Minnesota). Single crystals were attached to glass fibers and mounted on a Bruker SMART Platform CCD (tfpb$^-$ structures) or Siemens SMART Platform CCD (pftpb$^-$ structure) for data collection at 123 K (tfpb$^-$ structures) or 173 K (pftpb$^-$ structure) using graphite monochromated Mo Kα radiation ($\lambda = 0.71073$ Å). An initial set of cell constants was calculated from reflections harvested from three sets of 20 frames oriented such that orthogonal wedges of reciprocal space were surveyed. Final cell constants were calculated from at least 12443 strong reflections from the actual data collection. Data were collected to the extent of (1.5−2.0) hemispheres at a resolution of 0.84 Å using *φ*-scans. For all structures, the intensity data were corrected for absorption and decay using SADABS.[15] Solution and refinement were performed utilizing SHELXTL-V6.12.[16] The solvent accessible void space fraction was calculated for these structures using PLATON/VOID.[17,18] A description of how these calculations are performed has previously been presented.[10] The refinement for compound **3b** was not completed to convergence due to the extreme size of the unit cell that results in over 4000 parameters; however, this level of refinement is adequate to describe the connectivity and for void space calculations of sufficient accuracy. Further details concerning the refinement of this structure are given in the Supporting Information.

O_2 Sensing Apparatus and Procedure. The crystalline films used for gas sensing were prepared by placing small (∼1 mg) amounts of crystalline solid on the end of a 1/4″ diameter brass rod, followed by addition of a small drop of MeOH to partially dissolve the sample. Slow evaporation of the MeOH resulted in an adherent crystalline film. Additionally, at least one single crystal of each compound was tested for oxygen sensing to confirm that the films used for oxygen sensing experiments and the single crystals used for X-ray diffraction gave similar results. In all of these cases, the prepared samples were then placed into the apparatus based on a 1/4″ diameter cross swage tube fitting. A 375 nm LED source filtered through an interference filter is used for excitation through the center fiber of a "six around one" bifurcated fiber optic probe. The emission was collected through the six fiber channel and sent into an Ocean Optics USB-2000 spectrometer. Various mole fractions of oxygen in nitrogen were prepared with a gas handling system composed of mass flow controllers. The spectrometer, mass flow controllers, temperature and pressure monitors were interfaced to a computer to allow control of the unattended data acquisition via a custom Labview program.

The emission data collected were analyzed with a spreadsheet written in Microsoft Excel. Data from three cycles of spectra obtained at approximately 0.0, 0.10, 0.21, 0.25, 0.40, 0.50, 0.65, 0.80, 0.90, and 1.0 mol fractions (χ_{O_2}) of O_2 in N_2 were used for the Stern−Volmer plots. The oxygen concentrations for the Stern−Volmer plots ($I_0/I = 1 + K_{SV}\chi_{O_2}$) reported here are expressed in terms of mole fraction at the standard atmospheric pressure of Minneapolis−St. Paul, MN of 0.97 atm. The unitless K_{SV} values quoted herein may be converted to partial pressure units (atm^{-1}) by dividing by 0.97 atm. The acquisitions were at room temperature, approximately 21.8 ± 1 °C. Exact gas mole fractions were calculated by referencing the feedback voltage of the mass flow controllers to a calibration previously performed. The emission intensity was integrated across the entire peak and divided by the integrated LED intensity for each spectrum to give I_0 (intensity under nitrogen) and I (intensity at a given O_2 mixture). I_0/I was plotted vs oxygen mole fraction in nitrogen to yield a Stern−Volmer plot; a linear regression model was used to calculate the slope. The

(15) Blessing, R. H. *Acta Crystallogr., A* **1995**, *A51*, 33.
(16) *SHELXTL 6.12*; Bruker AXS: Madison, WI, 2001.
(17) Spek, A. L. *J. Appl. Crystallogr.* **2003**, *36*, 7.
(18) Spek, A. L. *PLATON, A Multipurpose Crystallographic Tool*; Utrecht University: Utrecht, The Netherlands, 2005.

Figure 1. (Left) Fiber optic probe (actual size) used for dissolved O_2 sensing. (Right) Tip of fiber optic with compound at 50× magnification.

Stern−Volmer slopes from multiple runs taken on separately prepared samples were averaged and the standard deviation was calculated.

Dissolved Oxygen Sensing Procedure. A crystalline film of the complex was deposited on the end of a fiber optic tip as shown in Figure 1. The tip is inserted into deionized water contained in a round-bottom flask. Illumination was gated so that the samples were only irradiated while data were being collected, not during purging time. The water is purged with mol fractions of O_2 in N_2 of 0.0, 0.10, 0.20, 0.50, and 1.0. Three cycles of spectra were taken. The resulting data were corrected for stray light, fit to the Stern−Volmer equation, averaged, and the standard deviation calculated. Because these data were collected in Seattle, WA which is at a significantly lower elevation (i.e., nominally at sea level), the unitless K_{SV} value that resulted was corrected so it could be directly compared with the K_{SV}'s calculated from data collected in Minneapolis, MN.

Solid-State Photophysical Measurements. The absolute solid-state quantum yields of the compounds were obtained by a modification of the method described by Wrighton et al.[19] A Fluorilon scattering target was used instead of MgO. The methods used to obtain and correct the data for detector response have been described previously.[3] Corrected spectra of **1**, **2b**, **3b** and **3c** are shown in the Supporting Information. Solid-state emission lifetimes were obtained with an in-house constructed circuit that pulses a 400 nm LED for excitation of the sample. The light was conducted through one leg of a bifurcated fiber optic probe to the sample housed in a sample compartment identical to the one used for the Stern−Volmer measurements. The emission decay and scattered light were collected by the other fiber optic leg, filtered through a cut off filter to remove the scattered excitation light and conducted to a Hamamatzu R928 PMT. The PMT signal was digitized by a sampling digital oscilloscope (Phillips PM 3323) interfaced to a computer running a LabView program similar to the one used for control of the Stern−Volmer data collection system. The lifetimes for compounds **1**, **2b**, and **3b** were modeled with a single exponential over 6 natural logarithm units; compound **3c** required a double exponential fit. More details concerning the lifetime data acquisition and processing have been presented previously.[3]

The pressure jump experiments were performed utilizing the same swage lock cross cell as described above. In this case, the input gas stream was from a compressed air tank and the pressure inside the cell was controlled with the regulator on the air tank. After pressurization, the system was tested to be leak free with the inlet and outlet valves closed. The time constant for pressure leaking out of the cell back to 1 atm ambient was measured by pressurizing the cell to 2.28 atm, closing the inlet valve and then monitoring the rate of the pressure drop back to 1 atm with a computer interfaced pressure transducer[20] when the outlet valve was opened. The full return time constant was approximately 40 ms, with a 50% return in 15 ms. A similar method was used to measure the time evolution of the emission spectrum except the OceanOptics spectrometer was used to collect emission spectra before and during the pressure release. Spectra could be collected to disk every 7 ms. The total emission intensity for each spectrum was calculated and the normalized intensity $[(I_p - I_{p0})/(I_\infty - I_{p0})]$ vs t was plotted for compounds **2b**, **3b**, and **3c**.

Results and Discussion

Molecular Oxygen Sensing. As discussed in the introduction we selected [Cu(POP)(dmp)]tfpb (**1**), as an initial candidate for an improved Cu(I) based oxygen gas sensor. A sample of this compound was synthesized in good yield, crystallized from methanol/water, and found to be pure via NMR and mass spectrometry. Crystalline films of **1** were found to sense O_2, but unfortunately the performance of these films significantly degraded in both emission intensity and in O_2 sensing ability during the preliminary studies (∼40% after 12.5 h alternating between 300 s exposures to N_2 and O_2). When not exposed to the LED, no degradation of performance occurs under either N_2 or O_2 consistent with a photoinduced origin of the degradation mode. To minimize this degradation during our measurements, the LED was gated off while waiting for the cell to equilibrate to the desired O_2 percentage, and was only gated on for the approximately 1 s required to obtain the luminescence spectrum. Using this methodology, a K_{SV} of 3.60(2) was found for compound **1**, which was about a 10-fold improvement over our previous best copper centered crystalline oxygen sensor.[10] Due to this encouraging result, we commenced additional compound design, synthesis and testing to minimize the performance degradation.

The previous demonstration and calculation that significant distortions in the coordination sphere angles of [Cu(dppe)(phen)]PF_6 (dppe = 1,2-bis(diphenylphosphino)ethane) occur in the excited state,[21] suggested that a similar distortion available to the POP ligand complex might occur and damage the surface crystallinity of the sensor. In an attempt to restrict this distortion, we replaced POP with the more rigid 4,5-bis(diphenylphosphino)-9,9-dimethylxanthene (xantphos) ligand. A number of new compounds (**2a**−**3c**) containing xantphos were synthesized in good yield, crystallized from methanol/water, and found to be pure via NMR and mass spectrometry. The subsequent screening of these compounds for stability and O_2 sensing showed a significant amount of quenching by oxygen for compounds **2b** and **3b**. Luminescence spectra for a crystalline film of **2b** under several different oxygen concentrations in nitrogen are shown in Figure 2. Additionally the stability of all of the xantphos compounds under N_2 and O_2 is much improved versus the POP compound herein reported.[22] For example, we observed an 8% decrease in intensity and sensing ability for **2b** after 12.5 h of continuous illumination alternating between nitrogen and oxygen in 300 s increments. An additional experiment showed that the small amount of degradation occurred during the oxygen exposures. A Stern−Volmer study of the O_2 sensing for **2b** and **3b** gave high K_{SV} values of 5.65(8)

(19) Wrighton, M. S.; Ginley, D. S.; Morse, D. L. *J. Phys. Chem.* **1974**, *78*, 2229.
(20) Logger Pro software; Vernier Software & Technology: Beaverton, OR.
(21) Vorontsov, I. I.; Graber, T.; Kovalevsky, A. Y.; Novozhilova, I. V.; Gembicky, M.; Chen, Y.-S.; Coppens, P. *J. Am. Chem. Soc.* **2009**, *131*, 6566.
(22) Further discussion of a preliminary investigation of the performance degradation is included in the Supporting Information.

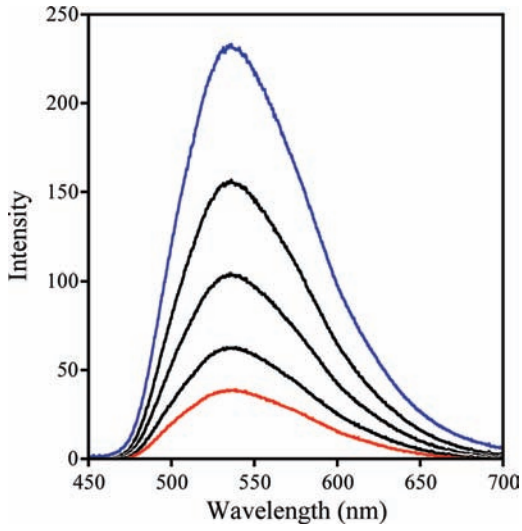

Figure 2. Uncorrected emission spectra for [Cu(xantphos)(dmp)]tfpb (**2b**) excited at 375 nm under varying concentrations of O_2 in N_2. The spectra under pure nitrogen and pure oxygen are shown in blue and red, respectively. Mole fraction of O_2 in N_2 from top to bottom is 0, 0.095, 0.241, 0.511, and 1.0.

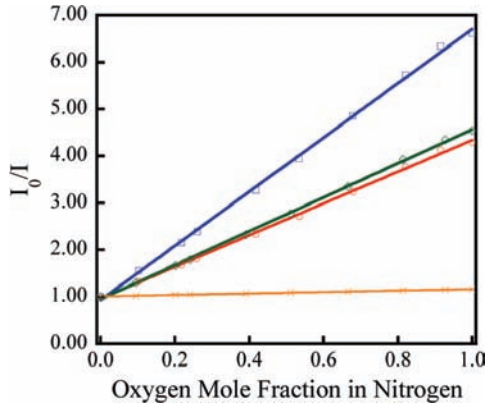

Figure 3. Stern−Volmer plots ((I_0/I) vs mole fraction of oxygen in nitrogen) for typical samples of **1** (green diamonds), **2b** (blue squares), **3b** (red circles), and **3c** (orange ×); the lines are the appropriate linear regression fits ($R^2 = 0.9994$, 0.9995, 0.9993, and 0.9996, respectively). Three cycles were collected over a 15 h period for each sample; one cycle is displayed for clarity.

and 3.41(9), respectively. Representative linear K_{SV} plots for **1**, **2b**, **3b** and **3c** are shown in Figure 3. A much smaller K_{SV} of 0.153(2) was found for compound **3c**, a perfluoro tetraphenyl borate salt with the same cation as **3b**. We also found that the precursor xantphos BF_4^- salts are oxygen sensors but they gave inconsistent results from sample to sample, including crystals taken from the same crystallization vial, leading to K_{SV} values with high standard deviations (0.7(4) for **2a** and 4(2) for **3a**). Due to this inconsistency further studies with the BF_4^- salts were not performed.

In contrast the standard deviations of the K_{SV} measurements for **2b**, **3b**, and **3c** are much smaller (see Table 2). They encompass three determinations each of three different samples prepared and measured in a similar manner over a period of up to 5 days. A few samples that were stored in air for several weeks after casting were measured and found to have Stern−Volmer plots virtually identical to those measured directly after film casting. Samples of some of the compounds that were stored in laboratory air for up to a year gave sensing determinations virtually identical to samples prepared and used immediately. The identical sensing abilities of single crystals of each of the compounds compared with the respective crystalline film measurements show that the films have the same crystal structures. For compound **2b** three different samples were illuminated with a 375 nm LED for 300 s under O_2 prior to beginning the gated K_{SV} determinations. These three samples yielded a K_{SV} of 5.35(2) which is lower than the 5.65(8) measured for the nonirradiated samples, consistent with a small amount of degradation. The small deviation in K_{SV} values between the three irradiated samples indicates that the degradation is consistent and reproducible. Some additional experiments to unravel the nature of the performance degradation have been conducted but are inconclusive. A brief discussion of these results is given in the Supporting Information.

One of the possible applications of oxygen sensors of this type is in sensing dissolved oxygen in water. To test the efficacy of dissolved oxygen sensing a methanol film of **2b** was deposited on the tip of a fiber optic (Figure 1) and oxygen sensing studies were performed on dissolved oxygen dilutions in deionized water. The K_{SV} value of 5.67(5) was determined over three cycles and is identical within experimental error to the value found for gaseous oxygen sensing with the same compound, 5.65(8). This indicates that compounds of this type could readily be utilized for dissolved O_2 sensing.

The gas phase time response of each xantphos Cu(I) sensor was measured by pressure jump experiments. Compounds **2b** and **3b** were of most interest and are plotted in Figure 4 for comparison. A very fast response (95% return at 0.051(4) s and 50% return at 0.022(6) s) for **2b** was observed, while compound **3b** had a slower response time (95% return at 0.71(2) s and 50% return at 0.044(3) s). These results are consistent with the presence of more void space in compound **2b** than **3b** (vide infra), which leads to more rapid oxygen diffusion in the crystal structure of compound **2b**.

Photophysics. Previously the photophysics of cations of the form $[Cu(POP)(NN)]^+$ in dichloromethane at room temperature have been reported.[11,23] We adopt the previous assignment (MLCT Cu(I) → phen) for the strong absorption and subsequent emission observed for these compounds.[23] The properties of the $[Cu(POP)(dmp)]^+$ cation have been reported as both $\phi =$

Table 2. Summary of Crystallographic, Photophysical and Oxygen Sensing Data

compounds	K_{SV}[a]	λ_{max} (nm)[b]	ϕ (N_2)[c]	ϕ (O_2)[d]	τ_0 (μs, N_2)[e]	τ (μs, O_2)[f]	% void space[g]
[Cu(POP)(dmp)]tfpb (**1**)	3.60(2)	517	0.88(9)	0.19(2)	26.0	6.4	4.6%
[Cu(xantphos)(dmp)]tfpb (**2b**)	5.65(8)	540	0.66(5)	0.084(3)	30.2	5.0	3.3%
[Cu(xantphos)(dipp)]tfpb (**3b**)	3.41(9)	513	0.95(5)	0.22(1)	38.5	9.6	2.0%
[Cu(xantphos)(dipp)]pftpb (**3c**)	0.153(2)	514	0.47(4)	0.31(3)	19.5[h]	15.6[h]	2.0%

[a] Estimated limit of detection is 5×10^{-3}. [b] Corrected solid-state emission peak wavelength. [c] Solid-state emission quantum yield under nitrogen. [d] Solid-state emission quantum yield under oxygen. [e] Solid-state emission lifetime under nitrogen. [f] Solid-state emission lifetime under oxygen. [g] Calculated percentage of solvent accessible void space from X-ray crystal structure. [h] weighted τ_m based on biexponential fit, see Supporting Information for details.

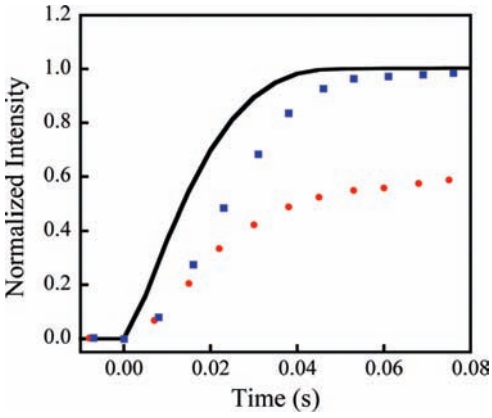

Figure 4. Normalized data from pressure jump experiment performed on [Cu(xantphos)(dmp)]tfpb (blue squares) and [Cu(xantphos)(dipp)]tfpb (red circles) with 375 nm LED excitations. 95% return at 0.051(4)s and 50% return at 0.022(6)s for [Cu(xantphos)(dmp)]tfpb and 95% return at 0.71(2)s and 50% return at 0.044(3)s for [Cu(xantphos)(dipp)]tfpb. The response of a pressure transducer is shown as a black line with 95% return at 0.035 s and 50% return at 0.015 s.

0.15, $\tau = 14.3$ μs[11,23] and $\phi = 0.09$, $\tau = 4.62$ μs[24] in a dichloromethane solution at room temperature and can be compared to the solid state measurements for **1** ($\phi = 0.88(9)$, $\tau = 26.0$ μs). The larger quantum yield and longer lifetime observed for **1** are consistent with a significant decrease in the nonradiative decay rates for the luminescence of the cation in the solid phase.

In addition to a large K_{SV} value, useful oxygen sensors based on LED excitation and photodiode detection must have a high emission quantum yield granted by favorable photophysical properties. Compounds **1**, **2b**, **3b**, and **3c** studied herein had excellent quantum yields (Table 2). In particular compound **3b** has an extremely high quantum yield under N_2, with a value near unity (0.95(5)). Compared to bis-phen systems these quantum yields under N_2 are over 5 times higher[10] and would allow the construction of usable sensors with smaller amounts of the sensor compound and less expensive and sophisticated detectors and excitation sources.

In a previous paper we discussed the equation that determines the magnitude of the K_{SV} constant in terms of the lifetime and oxygen permeability.[10] For a given oxygen permeability (which is controlled by the solid state structure) the K_{SV} should be directly proportional to the lifetime so increasing it is of paramount importance. The solid-state luminescence lifetimes (Table 1) of compounds **1**, **2b**, **3b**, and **3c** were determined as previously described and were found to be approximately ten times larger than those of comparable bis-phen systems.[10] For example, the best sensor compound (**2b**) has a lifetime of 30.2 μs under a nitrogen atmosphere. This 10-fold increase in lifetime is consistent with the approximately 10-fold increase in K_{SV} observed for compounds **1**, **2b**, and **3b**; compounds with significant void space. A cursory examination of the effect of oxygen on the emission lifetime was also performed (Table 1). Representative plots of $\ln(I_0/I)$ vs time for compound **2b** under pure nitrogen and pure oxygen are shown in Figure 5. All four compounds exhibit significantly shortened lifetimes under pure

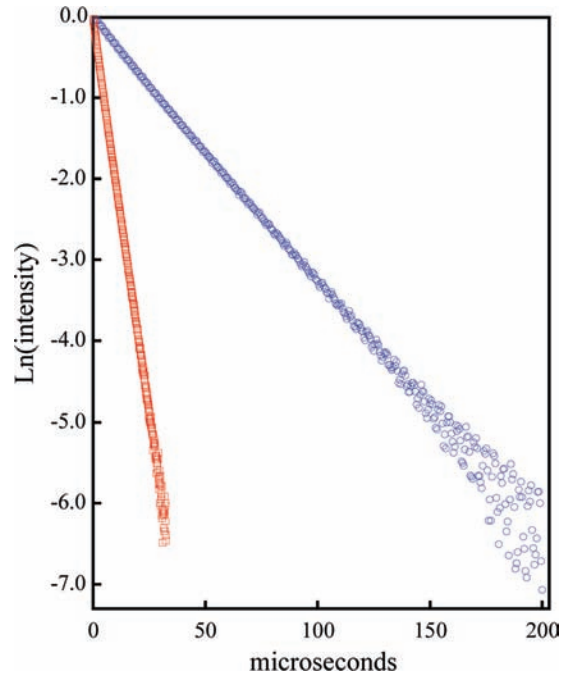

Figure 5. Plots of the natural log of the normalized emission intensity ($\ln(I_0/I)$) vs time for crystals of [Cu(xantphos)(dmp)]tfpb (**2b**) under nitrogen (blue circles, $\tau = 30.2$ μs) and oxygen (red squares, $\tau = 5.0$ μs).

oxygen, as expected. The "two point" K_{SV} values calculated from the lifetimes under pure nitrogen and pure oxygen are approximately 13% lower than those measured by the more accurate emission intensity quenching method. We believe that this diminution could result from some static quenching or from an increase in the light penetration depth at the longer wavelength (400 vs 385 nm) used for the lifetime experiments. Further experiments beyond the scope of the studies reported here will be needed to address this mechanistic detail.

Crystal Void Space and Oxygen Sensing. As outlined in the Experimental Section the solvent accessible void space (expressed as a fraction of the unit cell volume) was calculated for each crystal structure and is given in Table 1. Consistent with our previous hypothesis[10] that void space is a necessary but not sufficient condition for oxygen sensing in this type of compound, all four structures contain some void space and are oxygen sensors but the variations in the observed K_{SV} again suggest that the quality of the void space is also an important factor in determining the relative sensing ability. Closer examination of the crystal structure of the best sensor compound **2b** (illustrated in Figure 6) show that the void cavities, although not clear channels, are lined with and separated by highly mobile CF_3 groups, some of which are still severely disordered even at temperatures as low as 123 K. Similar situations exist for the other two sensor compounds **1** and **3b** (illustrated in the Supporting Information), whereas the poorest oxygen sensor (**3c**) contains void space restricted to distinct pockets. As in the previous studies, we suggest that the thermal activation of the CF_3 groups cluttering potential inter void space apertures can allow enough motion for solution like oxygen diffusion through the crystal and subsequently enable significant oxygen quenching.[10]

Conclusions

We have demonstrated that crystals of the emissive heteroleptic copper compounds **1**, **2b**, **3b**, and **3c** can sense molecular

(23) Kuang, S.-M.; Cuttell, D. G.; McMillin, D. R.; Fanwick, P. E.; Walton, R. A. *Inorg. Chem.* **2002**, *41*, 3313.
(24) Armaroli, N.; Accorsi, G.; Bergamini, G.; Ceroni, P.; Holler, M.; Moudam, O.; Duhayon, C.; Delavaux-Nicot, B.; Nierengarten, J.-F. *Inorg. Chim. Acta* **2007**, *360*, 1032.

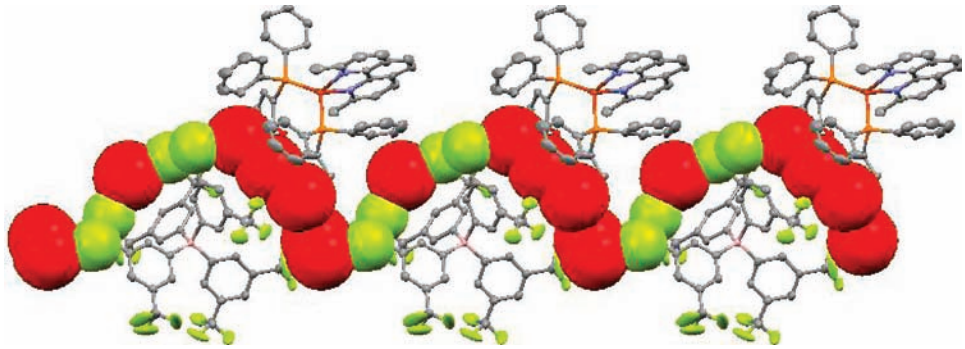

Figure 6. Depiction of the calculated void space as red space filling spheres for compound 2b. The fluorines of the disordered CF_3 groups that abut and clutter the void cavities are shown in green.

oxygen that is either in the gas or solution phases. The sensing ability correlates with the amount of void space calculated from the crystal structures. The linear Stern−Volmer plots with reproducible K_{SV} constants observed from sample to sample reinforce the observations that the sensing materials are crystalline and the sensing sites are homogeneous within the crystals. The long lifetimes, high quantum yields, appreciable K_{SV} values and very rapid response times (~30 μs, 0.66, 5.65, and 51 ms 95% return constant, respectively, for compound **2b**) for these compounds are significantly better than our best previously studied copper O_2 sensor [Cu(dipp)$_2$]tfpb (with a K_{SV} value of 0.299).[10] The best of the new compounds reported here is more sensitive than the best crystalline ruthenium system ([Ru(4,7-Me_2phen)$_3$](tfpb)$_2$, 4.76K_{SV}) we previously reported.[3] Perhaps of additional technological importance, copper is significantly less expensive than ruthenium and compound **2b** can be synthesized from commercially available starting materials in a single step. As we have previously pointed out, the strictly linear Stern−Volmer behavior observed for this system and the absence of a polymer matrix that causes variability in sensor to sensor sensitivity allow, in principle, a simple single reference point calibration procedure, an important consideration for an inexpensive onetime limited use sensor that would be mass produced.

Of final concern is the degradation in performance exhibited by these compounds that might limit their commercial usefulness for long-term sensing applications. For short-term disposable applications, the degradation may not be a significant issue. For example, if an O_2 sensing device was built to utilize an LED with similar intensity to those used for our sensing data collection, we have calculated that a 1 s exposure time for a single sensing event near the ambient oxygen partial pressure in air would allow over 5000 measurements before a 1% error would be introduced due to degradation. This approximate calculation uses the 8% intensity decrease over 12.5 h of continuous irradiation with alternating nitrogen and pure oxygen discussed earlier. The high reproducibility of the degradation could allow it to be built into the sensor's data handling model to further extend the useable life of the sensor by at least another factor of 10 (50 000 measurements). For applications requiring continuous monitoring at ten measurements per minute, this would give a useable sensor life of approximately 3.5 days. If the sensed gas was lower in oxygen concentration than air, even more samples and an even longer usability parameter could be obtained within the 1% error limit. Future studies are in progress to obtain even more stable Cu containing materials that would retain the other desirable sensor characteristics discussed here.

Acknowledgment. This work was supported by the Center for Analytical Chemistry at the University of Washington and the Initiative for Renewable Energy and the Environment at the University of Minnesota. The authors thank Dr. Victor G. Young Jr. of the University of Minnesota X-ray crystallography laboratory and Dr. Kari A. McGee for assistance with some of the crystal structures.

Supporting Information Available: A discussion of the lifetime modeling for compound **3c**, crystal structure refinement details, a discussion of the unusual ^{1}H NMR of the dipp complexes, a cursory investigation of the performance degradation, data from the pressure jump experiment for compound **3c**, corrected solid-state luminescence spectra for **1**, **2b**, **3b**, and **3c**, and the void space diagrams for **1** and **3b**. This material is available free of charge via the Internet at http://pubs.acs.org.

JA103112M